IET Communications

WILEY

The Institution of Engineering and Technology

ORIGINAL RESEARCH OPEN ACCESS

A Microstrip Monopole Antenna Design for 5G Sub-6 GHz Applications Using Deep Learning

Berker Çolak[1] | Mehmet Ali Belen[1] | Farzad Kiani[2] | Ozlem Tari[3] | Peyman Mahouti[4] | Oguzhan Akgol[1,5]

[1]Department of Electrical and Electronics Engineering, Iskenderun Technical University, Hatay, Türkiye | [2]Data Science Application and Research Center (VEBIM), Fatih Sultan Mehmet Vakif University, Istanbul, Turkey | [3]Department of Mathematics and Computer Science, İstanbul Arel University, Istanbul, Turkey | [4]Department of Electronics and Communication Engineering, Yıldız Technical University, İstanbul, Turkey | [5]Department of Electrical and Communication Engineering, United Arab Emirates University, Al Ain, UAE

Correspondence: Oguzhan Akgol (oakgol@uaeu.ac.ae)

Received: 13 May 2025 | **Revised:** 3 November 2025 | **Accepted:** 13 November 2025

ABSTRACT

This study presents the design and optimization of a microstrip monopole antenna for 5G sub-6 GHz applications, employing a deep learning-based surrogate model combined with honeybee mating optimization (HBMO). The studied antenna structure employs air via arrays, intended to enhance antenna performance, including improved impedance matching and increased bandwidth. It is important to note that, unlike conventional antennas, the proposed design does not include a fully enclosed metallic cavity similar to a substrate integrated waveguide (SIW) antenna designs. A sensitivity analysis was conducted to assess the impact of these parameters, emphasizing the need for optimal tuning. To generate training and test datasets efficiently, Latin hypercube sampling (LHS) was used. A convolutional neural network (CNN) surrogate model was trained, outperforming other machine learning (ML) algorithms in predictive accuracy and generalization. The proposed CNN-HBMO framework reduced computational costs by minimizing the need for expensive electromagnetic (EM) simulations, enabling rapid design space exploration. The optimized antenna was fabricated and validated through experimental measurements, achieving 2–3 dBi gain and $S_{11} < -10$ dB across the 2.7–5.2 GHz band. Compared to existing designs, the proposed antenna offers a compact size (34×34 mm) with competitive performance, making it suitable for multi-band 5G applications.

1 | Introduction

Microstrip monopole antennas are a class of printed antennas (essentially planar monopoles) known for their simplicity and versatility in modern wireless systems. A microstrip monopole typically comprises a conductive patch or element printed on a dielectric substrate above a ground plane and it behaves electrically as a quarter-wavelength radiator. Owing to their planar form, these antennas are light, low-profile, inexpensive to fabricate, and straightforward to integrate into printed circuit boards or device enclosures. When properly engineered, they can also realize broad impedance bandwidths, which makes them suitable for multiband and wideband use such as Wi-Fi, LTE, IoT nodes, and 5G platforms [1].

For 5G specifically, sub-6 GHz (mid-band) operation is an attractive regime: it offers high data rates together with wider coverage and better penetration than mmWave, where sub-6 GHz microstrip monopoles compact can achieve a balance between electrical performance and physical footprint, making them a suitable solution candidate for smartphones, CPE units, and small cells [2]. Despite these advantages, meeting stringent 5G sub-6 GHz requirements is non-trivial, where the designers must secure wide operational bandwidth while keeping size compact and gain adequate. Because antenna size often trades off against bandwidth and efficiency, the monopole geometry (e.g., radiator shape, feed configuration, ground modifications) must be tuned carefully to support broad or multiple bands without degrading radiation behaviour. Miniaturization frequently

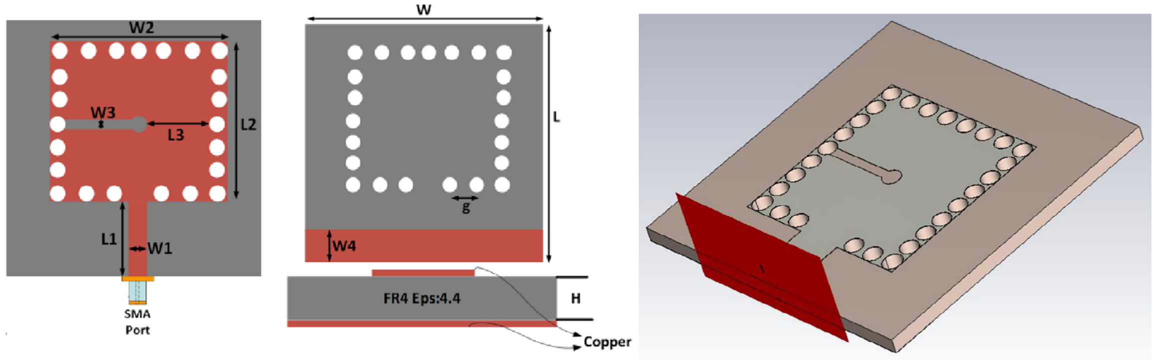

(a) (b)

FIGURE 1 | (a) Schematic; and (b) 3D CST model, of the proposed microstrip SIW-like antenna.
Note: w1–w4 and L1 L2 L3 correspond to the geometrical dimensions of the antenna indicated in Figure 1.

exacerbates these issues, inviting lower radiation efficiency, bandwidth narrowing, or detuning from nearby components [3]. Conventional workflows address these goals through iterative parameter sweeps and full-wave EM simulations (e.g., CST, HFSS), adjusting features such as patch contours, feed location, and ground slots to satisfy bandwidth and gain targets. While effective, this manual trial-and-error process becomes time-consuming and computationally costly for multiband layouts or high-dimensional design spaces [4].

To mitigate these burdens, recent work increasingly employs surrogate modelling and machine-learning-based design aids [5], where surrogate models trained on datasets pairing antenna geometries with simulated responses, such models—often neural networks—learn the nonlinear mappings from geometric parameters to metrics like S-parameters, gain, and bandwidth. Once trained, they provide near-instant performance estimates for new designs, enabling rapid exploration of the design space and supporting inverse design, i.e., searching for geometries that realize specified targets. Numerous studies report the effectiveness of this strategy in accelerating antenna design without sacrificing accuracy [5].For instance, Zhang et al. developed a deep neural network (DNN) surrogate model combined with an adaptive genetic algorithm to optimize a microstrip antenna array; this method dramatically accelerated the search for an optimal design that met multi-band performance targets, compared to brute-force simulation-based optimization [6]. By leveraging deep learning-based surrogate models, engineers can more readily achieve the wide bandwidth, high efficiency, and compact size needed for microstrip monopole antennas in 5G sub-6 GHz applications. Indeed, ML is proving to be a powerful tool to complement traditional antenna engineering, enabling rapid optimization in high-dimensional design spaces that would be impractical to explore with conventional techniques. This paper aims to present a monopole microstrip antenna and its design optimization procedure using artificial intelligence-based optimization methods to achieve an antenna design with high EM performance measures suitable for 5G and sub-6 GHz applications. The proposed approach not only provides an accelerated design optimization procedure but also allows designers to achieve the global optimal design in the vast search space without considering the computational cost of using EM simulation tools, where in some cases such search becomes infeasible. The rest of this paper is organized as follows. Section 2 provides information on antenna design. Section 3 presents the experimental and benchmark results. The conclusion and the future works will take place in the last section.

2 | Methodology

2.1 | Design of Antenna

In this section, general information about the antenna design is presented. The antenna (Figure 1) is modeled in a 3D EM simulation tool CST. The simulations are done using time domain solver, hexahedral FIT, Accuracy of —40 dB, with cells per wavelength of 15, fraction of maximum cell near to model equal to 20. The structural components ($x = [w1\ w2\ w3\ w4\ L1\ L2\ L3\ g]^T$) that determine the performance of the antenna are presented schematically in Figure 1 for the both top and ground layer of the antenna design. The design involves a series of variables, each of which plays a significant role in determining the scattering parameter (S11) response. Minor variations in these parameters can lead to a significant change in the antenna's EM response effecting its resonance frequency, impedance matching, and overall efficiency. It must be explicitly noted that, despite utilizing air vias (non-metallized through-holes) metallic vias arranged in patterns resembling SIW structures, the proposed antenna does not constitute a fully enclosed SIW cavity. The air vias are strategically placed to enhance EM performance parameters, such as bandwidth, impedance matching, and radiation efficiency, inspired by proven advantages observed in SIW designs.

To investigate the effect of these variables, a sensitivity analysis was performed on a selected set of critical design parameters, as depicted in Figure 2. During the sensitivity analysis, seven of the variables are taken as constant and equal to their middle values define in the range presented in Table 1, while the selected design parameter value is swept between the lower and upper variation limit. The sensitivity analysis shows that each parameter has a significant effect on the antenna's scattering parameter response, which ensures that selecting optimal parameter values is the key element to achieve the desired performance. However, due to the complex interdependencies among these parameters, determining the optimal design values have become

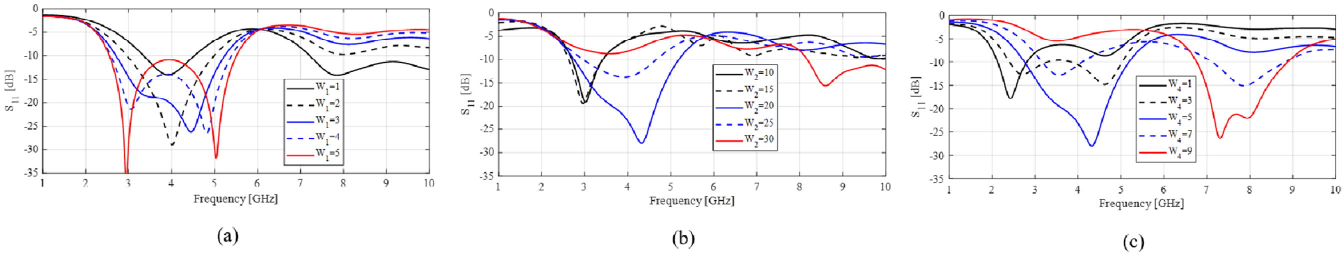

FIGURE 2 | Parametric analysis of (a) w_1; (b) w_2; and (c) w_4 all in [mm]. All other variables are taken as constant and middle value for each variables lower and upper variation limits given in Table 1.

TABLE 1 | Design variables and their range of variations in [mm].

Parameter	Lower	Upper	Parameter	Lower	Upper
w1	1	5	L1	5	15
w2	10	30	L2	10	30
w3	0.5	2	L3	2	10
w4	2	10	g	1	5

TABLE 2 | An example sample point ready to use for surrogate model from parametric analyses given in Figure 2.

Input parameter									Output parameter
w1	*w2*	*w3*	*w4*	*L1*	*L2*	*L3*	**g**	*f* [GHz]	S_{11} [dB]
1	20	1.25	6	10	20	6	3	1.0	−1.27
3	10	1.25	6	10	20	6	3	2.7	−9.98

a challenging endeavour. Herein, an optimization framework assisted by a deep learning-based surrogate model is proposed as a computationally efficient solution for this challenge. The surrogate model predicts the nonlinear relationships between the design parameters and the scattering response, enabling a more efficient search for optimal solutions in the given search space. By leveraging this approach, the computational burden associated with conventional optimization methods using direct EM simulation tools is significantly reduced [7, 8].

2.2 | Surrogate-Model Framework

In Table 1, the design variables and their respective ranges of variation are presented. Considering the multidimensional nature of the design space, employing a straightforward linear sampling approach for all variables is computationally infeasible since the exhaustive sampling of such a high-dimensional space would incur substantial computational costs, making it impractical for building a data-driven surrogate model [9]. To overcome this challenge, LHS [10–12] is employed for generating the training and test datasets. Thus, by this means, the entire design space is explored efficiently by stratifying the sample points to cover all ranges of the design variables without redundancy. Using this technique, 2000 samples are generated for training the surrogate model, while an additional 100 samples are reserved for testing (hold-out). This sampling strategy not only mitigates the computational burden but also ensures a diverse and representative dataset, which is essential for training a deep learning-based surrogate model with globally accurate prediction performance. In the next section, the generated training and test samples, Table 2, will be given to a series of ML algorithms to create counterpart surrogate models to the proposed deep learning approach.

Once the sample sets are available, a CNN is trained as the primary surrogate and embedded inside a HBMO framework, please check Table 3 for pseudo code representation of the frame work. Replacing the 3-D full-wave solver (≈ 2–3 min per simulation) with the CNN predictor (≈ 0.8 ms on a single CPU core) reduces the cost of one fitness evaluation by more than three orders of magnitude. Because HBMO typically requires 10^4–10^5 fitness calls to reach convergence in an eight-dimensional search space, the end-to-end wall time is shortened from several CPU-days to under half an hour on a desktop workstation—a level compatible with routine design iterations and industrial turn-around times. A surrogate cannot be adopted blindly, however; its predictive fidelity must be quantified against alternative regression engines to guarantee that the acceleration does not come at the expense

TABLE 3 | Pseudocode of CNN-HBMO surrogate optimization.

```
Input: design bounds 𝔅, band [f_L, f_U], N_train, N_test, max_Iter, k
Output: best design x*
/* — Build initial surrogate — */
X ← Latin yhpercube(𝔅, Ntrain)   ▷ sample geometries
Y ← CST(X)   ▷ full-wave |S11| spectra
CNN ← TrainCNN(X, Y)
/* — HBMO search with surrogate — */
Pop ← InitPopulation(𝔅)   ▷ queens + drones
For iter = 1 … maxIter do
   Fit ← Evaluate(cnn, pop, f_L,f_U)   ▷ uses surrogate only
   Pop ← HBMOstep (pop, fit)   ▷ mating + selection
   If iter mod k = 0 then   ▷ periodic truth updates
      Xv ← best (pop, m = 5)
      Yv ← CST (Xv)
      Append(X,Y; Xv,Yv); cnn ← FineTune (CNN, X,Y)
   End if
End for
Return argmin_{x∈Pop} evaluate (CNN, x, f_L, f_U)
```

TABLE 4 | Regression performance of each surrogate model for the studied antenna in RME [%]. All not mentioned HP are taken as default values in MATLAB 2023B.

Model	Optimal HP	K-fold	Test
Artificial neural networks-ANN [13]	# Hidden-layers: 2; # neurons: 20–35; Activation function: tansig; training method: Levenberg-Marquardt backpropagation	11.8	13.7
Support vector regression machine-SVRM [14]	Kernel function: Gaussian; Kernel scale: 0.85;	7.9	10.4
Gaussian process-GP [15]	Fit method: exact; Kernel function: squared exponential; predict method: bcd; block size BCD: 750	7.6	8.8
Convolutional neural network-CNN	# Hidden-layers: 4; # Neurons: 32–64–128–256; Activation function: Relu; training method: Adam; mini-batch size: 1000	3.2	4.7

of design accuracy. Accordingly, the same training/hold-out sets are supplied to three widely used counterparts, please check next section for more details, and their relative-mean errors (RME) on the 100 unseen samples are reported in the next section. This comparative study serves two purposes: (i) it justifies the choice of CNN as the most accurate and data-efficient surrogate for the present antenna topology; and (ii) it bounds the modelling error that propagates through HBMO, thereby ensuring that the final CST-validated design differs by less than 5 % from the surrogate prediction.

3 | Experimental and Benchmark Results

The antenna presented in this section utilizes a monopole microstrip-based design enhanced by an arrangement of air vias inspired by SIW technology. This inspired approach is adopted primarily to achieve enhanced EM performance attributes such as improved gain, impedance matching, and broader bandwidth characteristics, without employing a fully enclosed metallic SIW cavity. In this section, the generated training and test samples in the previous section will be given to a series of ML algorithms to develop alternative surrogate models [13–15] alongside the proposed deep learning-based approach. These ML algorithms will serve as benchmark models, allowing for a comprehensive comparison of their performance in predicting the scattering parameter response and facilitating the antenna design process where their performance will be evaluated based on their accuracy and ability to generalize across the test dataset. Then, the best-performing surrogate model will be selected to assist in the design optimization of the antenna for the targeted operational frequency band in order to achieve an optimization process in a more efficient manner by minimizing the need for costly direct EM simulation tool. This approach ensures that the optimal design parameters are identified accurately, achieving the desired antenna performance while maintaining computational feasibility [16]. Determining the appropriate hyper-parameters (HPs) for each surrogate model is critical to achieving optimal performance, therefore Bayesian Optimization was employed to fine-tune the HPs for each ML algorithm, ensuring a fair and systematic comparison [17, 18]. The optimization process allowed for a maximum of 45 evaluations and used 3-fold cross-validation to enhance the reliability of the results. The relative mean absolute error (RMAE) metric was used to evaluate both the training and test performance, helping to detect any signs of over-fitting. The evaluation results, summarized in Table 4, report the performance on both the training data (via K-fold cross-validation) and the test dataset.

In Table 4, the regression performance of various surrogate models employed for the studied antenna design, evaluated in terms of root mean error (RME) [%] for both K-fold cross-validation and test datasets. The table also includes the optimal hyper parameters (HP) for each model. The ANN model, with two hidden layers and 20–35 neurons per layer, uses the tansig activation function and is trained using the Levenberg-Marquardt back propagation algorithm. It achieves RME values of 11.8% and 13.7% for K-fold cross-validation and test datasets, respectively, while the SVRM model using a Gaussian kernel function with a scale of 0.85, the SVRM model exhibits RME values of 7.9% for K-fold validation and 10.4% for the test dataset, and the GP model employs an exact fit method, a squared exponential kernel function, and a block size of 750 for the prediction method. It delivers RME values of 7.6% and 8.8% for K-fold validation and test datasets, respectively. The CNN model, with four hidden layers (32–64–128–256 neurons) and a Relu activation function, is trained using the Adam optimizer with a mini-batch size of 1000. This model achieves the lowest RME values, with 3.2% for K-fold validation and 4.7% for the test dataset, demonstrating superior predictive accuracy compared to other models. These results highlight the CNN model's effectiveness in accurately capturing the antenna's performance metrics, making it a reliable surrogate model for the studied application. The performance metrics of each model underline the trade-offs between complexity, computational cost, and predictive accuracy, aiding in the selection of the most suitable surrogate model for antenna design optimization. Thus, the CNN surrogate model will be deployed for assisting the optimization procedure of the antenna.

After identifying the most suitable surrogate model—the CNN—for the antenna, the next objective is to leverage this surrogate to assist in the design optimization process. Despite the large search space and the multitude of potential solution candidates, using a surrogate-assisted optimization strategy is highly effective. This approach significantly reduces computational costs, as even with thousands of function evaluations, the total simulation time is reduced to just a few seconds. In contrast, performing direct EM simulations would require several minutes for a single function evaluation [19].

TABLE 5 | Optimal design variables obtained via hybrid HBMO-CNN search protocol all in [mm]. the selected material is FR4.

w	34	*L*	34
w1	2.85	*L1*	7.2
w2	19.5	*L2*	19.5
w3	0.95	*L3*	7
w4	4.97	*g*	2.59

In this work, HBMO, a meta-heuristic optimization method inspired by the mating behavior of honeybees, is employed. HBMO is a well-established optimization technique that excels in parallel processing and has proven to be highly successful in addressing similar microwave optimization challenges [20].

Here it must be emphasized that, although the selection of optimization algorithm is a crucial step in design optimizations. With the introduction of the deep-learning surrogate reduces the average EM response evaluation time from several minutes to well below one second. Making large-scale global optimization practical for the first time in antenna design. With this acceleration, we can afford populations on the order of 10^3 and iteration counts of 10^3—i.e. $\approx 10^6$ fitness calls—without exceeding a few minutes of wall-clock time on a standard workstation. Under such generous sampling, the performance gap that traditionally separates heuristic optimizers (HBMO, GA, PSO, differential evolution, hybrid models, etc.) all but disappears: each algorithm receives enough exploratory pressure to traverse the entire design space, avoid premature convergence, and land on the same globally optimal region. Consequently, optimization success becomes dominated not by the choice of search heuristic but by the fidelity of the surrogate itself.

The cost function, defined in Equation 1, guides the optimization protocol to determine the optimal parameter vector x, where $x = [w1\ w2\ w3\ w4\ L1\ L2\ L3\ g]^T$. By integrating the CNN surrogate model within the HBMO framework, the optimization process becomes more efficient, reducing the need for expensive EM simulations while ensuring accurate and effective exploration of the design space. $[f_L, f_U]$ are the lower and upper frequency values of the targeted operating bands under the parametric limitations of the geometric design variables. The optimally determined design variables of the antenna are presented in Table 5.

$$\mathbf{x}^{*} = \arg\min_{\mathbf{x}} \{ f \in [f_L, f_U] : |S_{11}(\mathbf{x}, f)| \} \tag{1}$$

For validation of the proposed approach, the obtained design is fabricated (Figure 3(a)) and its simulated results are compared with the experimental results (Figure 3(b, c)). Figure 3(b) illustrates the scattering parameter S_{11} characteristics of the proposed antenna design, showcasing both the measured results (black solid line) and the surrogate model predictions (red dashed line). The antenna demonstrates efficient operation within the 3–5 GHz frequency band, as evidenced by the S_{11} values dropping below the −10 dB threshold, which indicates effective impedance matching and minimal reflection. The surrogate model effectively predicts the S_{11} behaviour across the frequency range, closely approximating the measured data. Minor discrepancies between the measured and surrogate model curves, particularly around the resonant frequency, can be attributed to experimental uncertainties or simplifications in the surrogate model's assumptions. Nonetheless, the agreement between the two curves validates the surrogate model's reliability for analysing the antenna's performance. This result highlights the capability of the surrogate modelling approach to streamline the design and optimization process for antennas, particularly within the targeted 3–5 GHz operational band. The integration of such predictive tools in the

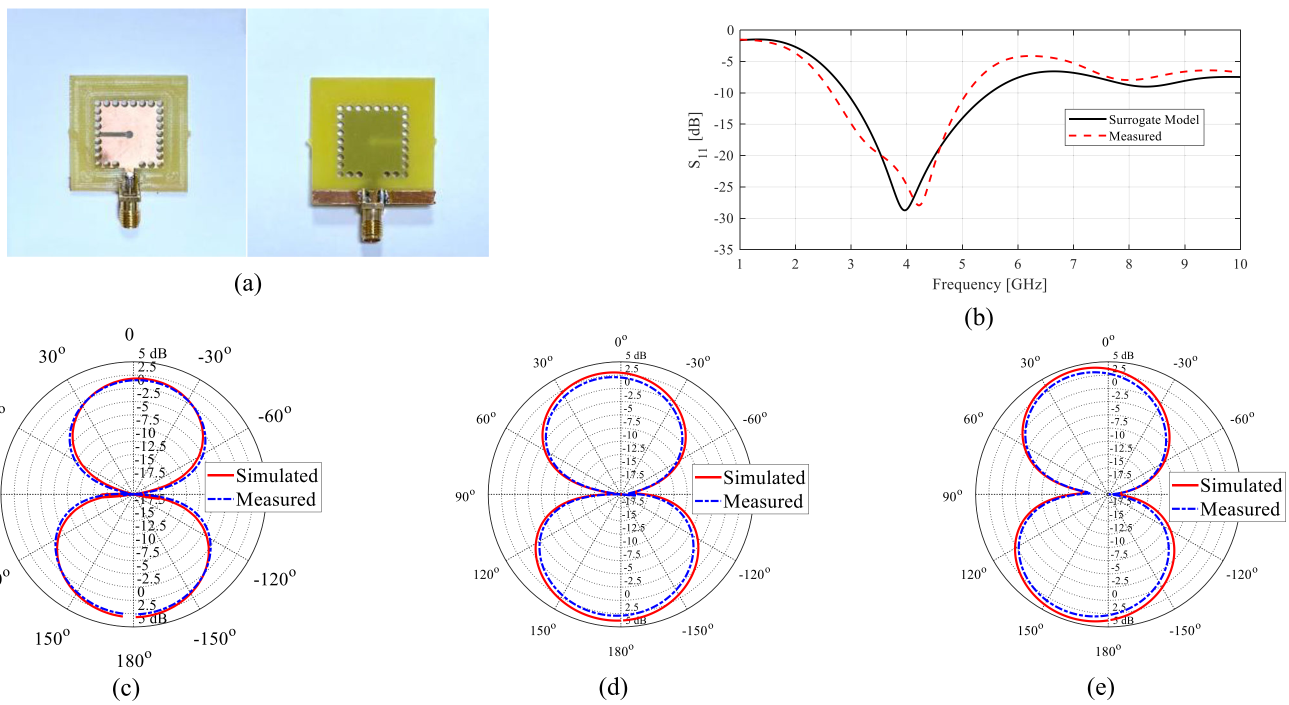

FIGURE 3 | (a) Prototyped antenna; measured (b) scattering parameter; radiation patterns at (c) 3 GHz; (d) 4 GHz; and (e) 5 GHz.

TABLE 6 | Performance comparison of the proposed approach to the counterpart work from the literature. NA: Not Available. The frequency for calculation of wavelength is taken equal to the center frequency of the operation band in each example.

Methods	Frequency [GHz]	S_{11} [dB]	Gain [dBi]	Material	Size [λ]
Proposed antenna	2.7–5.2	←10	2–3	FR4	0.77 × 0.77
[21]	2.24, 4.28, 5.5	←10	NA	FR4	0.58 × 0.36
[22]	3.6–4.1	←10	7.95	FR4	0.63 × 0.67
[23]	2.4	←15	10	PLA	2.21 × 1.87
[24]	4.1–8	←10	8–11	NA	1.24 × 1.24
[25]	4.8–8.53	←10	9.58	FR4	1.29 × 1.29
[26]	2–5	←10	3.1–5.1	FR4	0.58 × 0.58
[27]	0.64–2.2	←10	NA	Wangling TP-1	1.75 [diameter]
[28]	5.32–25	←10	7.8–13.8	ROGERS 5880	0.98 × 0.98
[29]	2.4, 5.8	←10	3.8–5.9	FR4	2.6 × 2.6

NA = Not Available. FR4, PLA, Rogers 5880 and Wangling TP-1 refer to the substrate materials used in the referenced designs.

design workflow significantly reduces the computational and experimental effort required, while maintaining high accuracy in performance prediction.

Figure 3(c) presents the radiation patterns of the proposed antenna design in polar plots for frequencies of 3 GHz, 4 GHz, and 5 GHz. The black solid lines correspond to the simulated results obtained from a 3D EM simulation tool, while the blue dotted lines represent the measured results from experimental testing. Here it must be mentioned that the proposed deep learning surrogate model is used to predict the S_{11} characteristic of the antenna and not the radiation characteristic. However, due to the nature of the design, the antenna has a high directivity, which allows the design to have a good radiation characteristic if the S_{11} is sufficiently good too. Thus, the simulated performance is obtained via using a 3D-EM simulation tool. As can be observed from the figure, the antenna demonstrates consistent agreement between the simulated and measured results across the frequency range. The radiation patterns exhibit a directional behaviour, with slight deviations between the simulated and measured data attributed to fabrication tolerances, measurement setup inaccuracies, or environmental factors affecting the experimental setup. These minor differences do not detract from the overall performance consistency. At 3 GHz (c), the simulated and measured patterns align closely, indicating robust antenna behaviour at the lower end of the operational band. At 4 GHz (d) and 5 GHz (e), the patterns remain similarly consistent, showcasing the antenna's effective performance across its operational range.

Moreover, Table 6 presents a performance comparison between the proposed antenna, optimized using the HBMO + CNN approach, and other antenna designs from the literature [21–26]. The comparison is made in terms of key EM performance metrics, including operating frequency range, scattering parameter (S_{11}), gain, antenna material, and size. The proposed antenna operates within a frequency range of 2.7–5.2 GHz, achieving an S_{11} value below –10 dB across the entire band, indicating excellent impedance matching. In terms of gain, the proposed design offers 2–3 dBi, which, while moderate, meets the desired specifications for the intended application. When compared to other designs, the following observations can be made: (I) the proposed antenna has a smaller size, 34 × 34 [mm], than most other antennas, making it advantageous for compact applications. For instance, antennas in [22] and [25] are significantly larger, with dimensions of 49 × 52 [mm] and 58 × 58 [mm], respectively; (II) while some designs, such as [23] and [25], achieve higher gain values (10 dBi and 9.58 dBi, respectively), this often comes at the cost of larger physical dimensions and materials such as PLA, which may not be suitable for all applications; and (III) the proposed antenna's frequency coverage is broader than several other designs, such as [21] and [26], which operate across more specific sub-bands that can offer more flexibility for multi-band applications.

Thus, based on the mentioned superiority of the proposed design compared to the counterpart works, it is safe to say that the proposed antenna design achieves a balance between size, gain, and bandwidth performance, which makes it suitable for applications that require compactness and good performance across a relatively broad frequency range. While other antennas may offer higher gain, the compact size of the proposed design provides significant advantages in terms of practical deployment.

4 | Conclusion

Herein, a monopole microstrip antenna was designed and optimized for 5G sub-6 GHz applications. This structure, while leveraging air via arrays arranged similarly to SIW antennas, distinctly does not employ the fully enclosed metal cavity of traditional SIW structures. Instead, air vias were used strategically to improve the EM performance of the microstrip antenna, achieving effective impedance matching and good radiation performance within a compact form factor. The optimization of the antenna for targeted 5G sub-6 GHz applications is achieved by using a deep learning-based surrogate model assisted optimization with HBMO. The proposed approach effectively addressed the complex challenges in antenna design by leveraging a CNN-assisted optimization strategy where the proposed combination not only reduced the computational burden associated with traditional EM simulations but also ensured achieving a highly accurate global surrogate model to be used for design optimization of the aimed antenna. The final optimization framework, utilizing the CNN-based surrogate model within the HBMO method, provided significant improvements in efficiency by reducing simulation time from minutes to seconds per function evaluation, which allowed for rapid exploration of the design space and effective optimization of the antenna's performance. The fabricated antenna, validated through experimental measurements, exhibited excellent impedance matching ($S_{11} < -10$ dB) across the 2.7–5.2 GHz frequency band and achieved a gain of 2–3 dBi, meeting the design requirements for compact and efficient 5G antennas. Compared to other designs from the literature, the proposed antenna demonstrated a competitive balance between size, bandwidth, and gain, making it well-suited for multi-band 5G applications.

Here, the proposed deep learning regression model-assisted optimization framework's accuracy is limited to the defined training data's range and bound to the quality of the data samples. The created model is only applicable to the studied antenna for the given variables and an alternation to the design or design variables range might have a severe effect on accuracy of the model, which can be only solved by providing new data samples for the mentioned alternation. However, due to the nature of deep learning methods, the new additional data can be used to improve the previously trained deep learning models performance. Thus, it is safe to say that the proposed approach which is achieved by the integration of deep learning-based surrogate modelling with meta-heuristic optimization techniques, provides a powerful and scalable approach for antenna design that is not only applicable to antennas but can also be extended to other complex microwave and antenna systems, offering a promising solution simulating expensive problems in the field of microwave engineering.

Author Contributions

Berker Çolak: conceptualization, data curation, formal analysis, investigation, methodology, software, writing – original draft. **Mehmet Ali Belen:** conceptualization, formal analysis, methodology, supervision, validation, visualization, writing – review and editing. **Farzad Kiani:** investigation, visualization, writing – review and editing. **Ozlem Tari:** formal analysis, investigation, validation, visualization, writing – review and editing. **Peyman Mahouti:** investigation, methodology, validation, visualization, writing – review and editing. **Oguzhan Akgol:** conceptualization, investigation, methodology, resources, validation, visualization, writing – review and editing.

Funding

This work is supported by the Yildiz Technical University for founding our research under project number FBA-2025-6780.

Conflicts of Interest

The authors declare no conflicts of interest.

Data Availability Statement

Data will be made available on request.

References

1. P. Pradeep, J. Kottareddygari, and C. Paidimarry, "Design of a Dual-Band Monopole Antenna for Internet of Things and Sub-6 GHz 5G Applications," in *2024 IEEE Wireless Antenna and Microwave Symposium (WAMS)* (2024), https://doi.org/10.1109/WAMS59642.2024.10528093.

2. U. Farooq, M. Nasir, A. Iftikhar, et al., "A Compact Monopole Patch Antenna for Future Sub 6 GHz 5G Wireless Applications," in *2020 IEEE International Symposium on Antennas and Propagation and North American Radio Science Meeting* (2020), https://doi.org/10.1109/IEEECONF35879.2020.9329624.

3. M. Fallahpour and R. Zoughi, "Antenna Miniaturization Techniques: A Review of Topology- and Material-Based Methods," *IEEE Antennas and Propagation Magazine* 60, no. 1 (2018): 38–50, https://doi.org/10.1109/MAP.2017.2774138.

4. M. Melo, P. Santos, E. Faustino, C. Bastos-Filho, and A. Sodré, "Computational Intelligence-Based Methodology for Antenna Development," *IEEE Access* 10 (2022): 1860–1870, https://doi.org/10.1109/ACCESS.2021.3137198.

5. S. Koziel and A. Pietrenko-Dabrowska, "Performance-Based Nested Surrogate Modeling of Antenna Input Characteristics," *IEEE Transactions on Antennas and Propagation* 67, no. 5 (2019): 2904–2912, https://doi.org/10.1109/TAP.2019.2896761.

6. J. Zhang, G. Xu, K. Jin, Y. Zou, K. Kang, and W. Yin, "Design and Optimization of Differentially Fed Microstrip Cross-Grid Array Antenna With DNN Surrogate Model-Enabled AGA," *IEEE Transactions on Antennas and Propagation* 73, no. 1 (2025): 241–253, https://doi.org/10.1109/TAP.2024.3474096.

7. N. Sarker, P. Podder, M. R. H. Mondal, S. S. Shafin, and J. Kamruzzaman, "Applications of Machine Learning and Deep Learning in Antenna Design, Optimization and Selection: A Review," *IEEE Access* 11 (2023): 103890–103915, https://doi.org/10.1109/ACCESS.2023.3317371.

8. P. Mahouti, A. Kızılay, O. Tari, A. Belen, and M. A. Belen, "Design Optimization of Ultra Wide Band Vivaldi Antenna Using Artificial Intelligence," in *2021 International Applied Computational Electromagnetics Society Symposium (ACES)* (2021).

9. A. Pietrenko-Dabrowska and S. Koziel, "Model Management for Low-Computational-Budget Simulation-Based Optimization of Antenna Structures Using Nature-Inspired Algorithms," *Applied Soft Computing* 154 (2024): 111356, https://doi.org/10.1016/j.asoc.2024.111356.

10. W. L. Loh, "On Latin Hypercube Sampling," *The Annals of Statistics* 24, no. 5 (1996): 2058–2080, https://doi.org/10.1214/aos/1069362310.

11. A. Uluslu, "Design of Microstrip Filter by Modeling With Reduced Data," *The Applied Computational Electromagnetics Society Journal (ACES)* (2021).

12. A. Uluslu, "Application of Artificial Neural Network Base Enhanced MLP Model for Scattering Parameter Prediction of Dual-Band Helical Antenna," *Applied Computational Electromagnetics Society Journal* 38, no. 5 (2023): 316–324.

13. A. Uluslu, "Additional Acceleration of Antenna Optimal Characterizationwith Modeling Support," *Applied Computational Electromagnetics Society Journal (ACES)* 39, no. 5 (2024): 396–404, https://doi.org/10.13052/2024.ACES.J.390503.

14. H. Drucker, C. J. Burges, L. Kaufman, A. Smola, and V. Vapnik, "Support Vector Regression Machines," *Advances in Neural Information Processing Systems* 9 (1996).

15. E. Schulz, M. Speekenbrink, and A. Krause, "A Tutorial on Gaussian Process Regression: Modelling, Exploring, and Exploiting Functions," *Journal of Mathematical Psychology* 85 (2018): 1–16, https://doi.org/10.1016/j.jmp.2018.03.001.

16. M. C. De Melo, P. B. Santos, E. Faustino, C. J. Bastos-Filho, and A. C. Sodré, "Computational Intelligence-Based Methodology for Antenna Development," *IEEE Access* 10 (2021): 1860–1870, https://doi.org/10.1109/ACCESS.2021.3137198.

17. R. Ortiz, P. Miranda-Chiquito, A. Encalada-Davila, et al., "An Enhanced Modeling Framework for Bearing Fault Simulation and Machine Learning-Based Identification With Bayesian-Optimized

Hyperparameter Tuning," *Journal of Computing and Information Science in Engineering* 24, no. 9 (2024): 091002, https://doi.org/10.1115/1.4065777.

18. P. A. Opoku, L. Shu, T. Ansah-Narh, et al., "Prediction of Karst Spring Discharge Using LSTM With Bayesian Optimisation Hyperparameter Tuning: A Laboratory Physical Model Approach," *Modeling Earth Systems and Environment* 10 (2024): 1457–1482, https://doi.org/10.1007/s40808-023-01828-w.

19. P. Mahouti, A. Belen, O. Tari, M. A. Belen, S. Karahan, and S. Koziel, "Data-Driven Surrogate-Assisted Optimization of Metamaterial-Based Filtenna Using Deep Learning," *Electronics* 12, no. 7 (2023): 1584, https://doi.org/10.3390/electronics12071584.

20. F. Güneş, S. Demirel, and P. Mahouti, "Design of a Front–End Amplifier for the Maximum Power Delivery and Required Noise by HBMO With Support Vector Microstrip Model," *Radioengineering* 23, no. 1 (2014): 134–143.

21. S. Salihovic and S. T. Imeci, "A Stub Microstrip Patch Antenna for Sub 6 GHz - 5G Applications," *Heritage and Sustainable Development* 5, no. 1 (2023): 99–106, https://doi.org/10.37868/hsd.v5i1.104.

22. M. A. Haque, M. A. Rahman, S. S. Al-Bawri, et al., "Machine Learning-Based Approach for Bandwidth and Frequency Prediction for N77 band 5G Antenna," *Physica Scripta* 99, no. 2 (2024): 026005, https://doi.org/10.1088/1402-4896/ad1d40.

23. M. A. Belen, "Stacked Micro-Strip Patch Antenna Design for ISM Band Applications With 3D-Printing Technology," *Microwave and Optical Technology Letters* 61 no. 3 (2019): 709–712, https://doi.org/10.1002/mop.31603712/BELEN.

24. B. Xie, R. Zhang, H. Wang, et al., "Broadband Metasurface Antenna With Size-Varying Square Patches," *Microwave and Optical Technology Letters* 65, no. 12 (2023): 3319–3325, https://doi.org/10.1002/mop.33867.

25. Y. Mao, H. Liu, S. Li, M. Zhu, and S. Zhang, "A novel Single-Layer Dual-Bandcircularly Polarized Metasurface Antenna Formaritime Communications," *Microwave and Optical Technology Letters* 66, no. 4 (2024): e34159, https://doi.org/10.1002/mop.34159.

26. S. Goswami, P. Borah, K. Sarmah, and K. K. Sarma, "Design of a Dual-Band Multilayer Antenna and its Equivalent Circuit Modeling With Vector-Fitting and Genetic Algorithm," *AEU-International Journal of Electronics and Communications* 138 (2021): 153838.

27. S. M. H. Mousavi, K. Sultan, L. Guo, A. S. Janani, K. Bialkowski, and A. M. Abbosh, "Dual-Sense Circularly Polarized Substrate Integrated Waveguide Antenna for Deep Torso Imaging," *IEEE Transactions on Antennas and Propagation* 73, no. 1 (2025): 188–200, https://doi.org/10.1109/TAP.2024.3509212.

28. M. M. He, Z. H. Tu, and N. Nie, "Dual-Band Dual-Circularly Polarized Aperture-Shared Antenna Based on SIW for Millimeter-Wave/Sub-6 GHz Communication Applications," *Microwave and Optical Technology Letters* 67, no. 3 (2025): e70163, https://doi.org/10.1002/mop.70163.

29. M. Rajaguru Kattiakara Muni Samy and A. Gudipalli, "Design of Compact Dual-Band Eighth-Mode SIW Antenna for On-Body ISM Band Application," *IEEE Access* 12 (2024): 145069–145078, https://doi.org/10.1109/ACCESS.2024.3472310.